ALS-causing SOD1 mutants generate vascular changes prior to motor neuron degeneration

Zhihui Zhong, Rashid Deane, Zarina Ali, Margaret Parisi, Yuriy Shapovalov, Kerry O'Banion, Konstantin Stojanovic, Abhay Sagare, Severine Boillee, Don W. Cleveland and Berislav V. Zlokovic

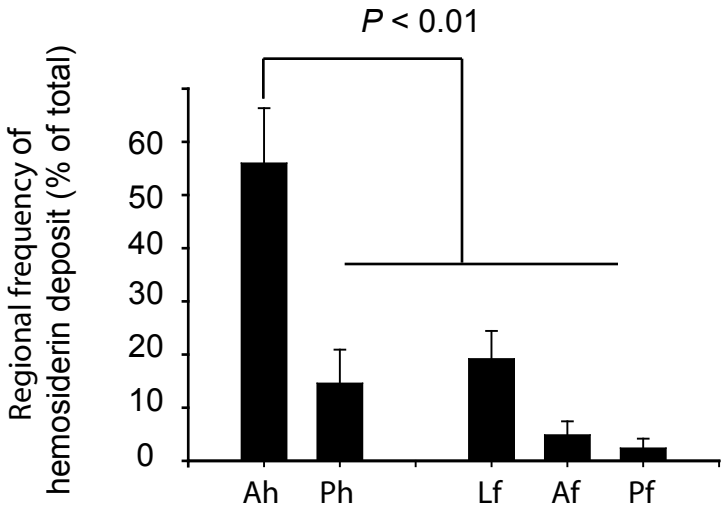

Supplementary Figure 1. Regional analysis of hemosiderin deposits in the lumbar spinal cord of SOD1^{G93A} mice presymptomatically.

Regional analysis of hemosiderin deposits in the anterior horn (Ah), posterior horn (Ph), lateral funiculus (Lf), anterior funiculus (Af) and posterior funiculus (Pf) of the lumbar spinal cord (L2–L5) of SOD1^{G93A} mice (2 month). Twelve nonadjacent sections (> 250 μm apart in L2–L5 region were examined from each mouse. Total number of Prussian blue-positive spots for hemosiderin was determined as described in the methods. Hemosiderin deposit frequency in Ah, Ph, Lf, Af and Pf regions was expressed as a percentage of total number of Prussian blue positive spots. Values are mean ± S.E.M, n = 4 mice.

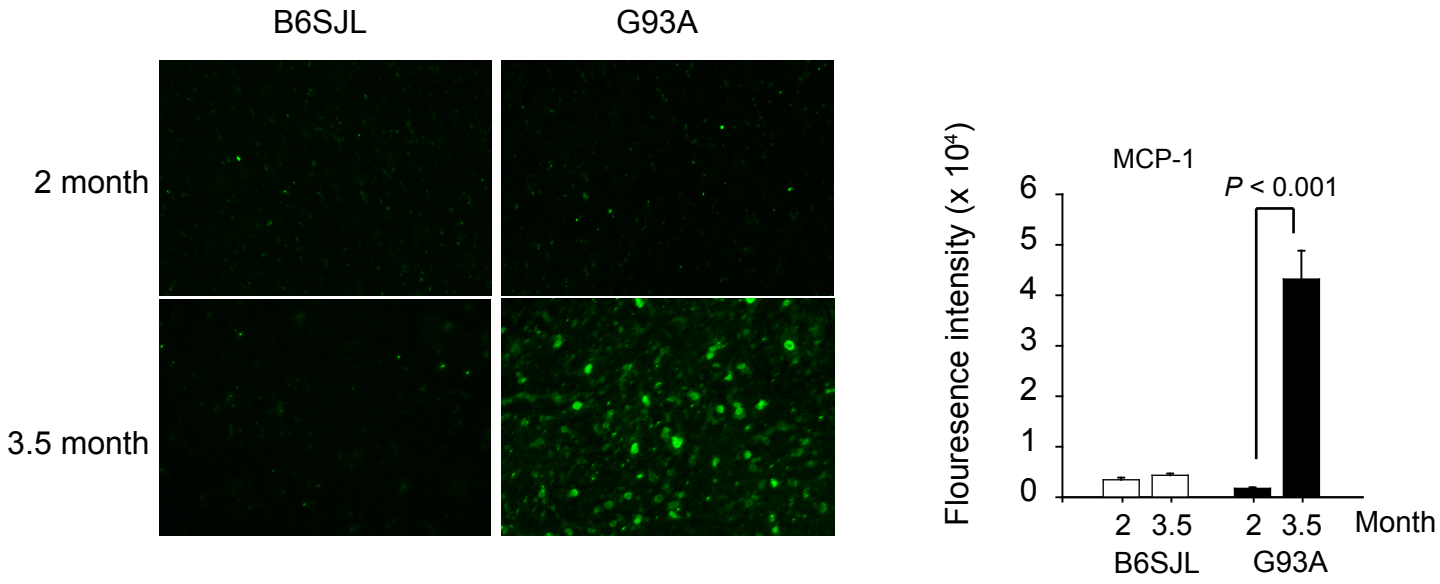

Supplementary Figure 2. MCP-1 immunofluorescent staining in the lumbar spinal cord of SOD1^{G93A} mice at presymptomatic and symptomatic stage.

Representative images of MCP-1 immunofluorescent staining on the lumbar spinal cord (L3) sections of SOD1^{G93A} and the age-matched littermate control B6SJL mice (2 and 3.5 months of age, n = 3–5 mice per group). Briefly, the 14 μm cryosections prepared as described in the method were blocked in 5% swine serum for 1 h at room temperature and probed using the affinity purified goat polyclonal anti-mouse MCP-1 (1:100, Santa Cruz Biotechnology, Santa Cruz, CA) for overnight at 4^{o}C. AlexaFluor 488 donkey anti-goat IgG (1:200, Molecular Probes, Eugene, OR) was used as a secondary antibody. Images were taken using an Olympus AX70 fluorescent microscope. Graph shows the comparison of fluorescence signal intensity for MCP-1 in the lumbar spinal cord of SOD1^{G93A} mice at different age.

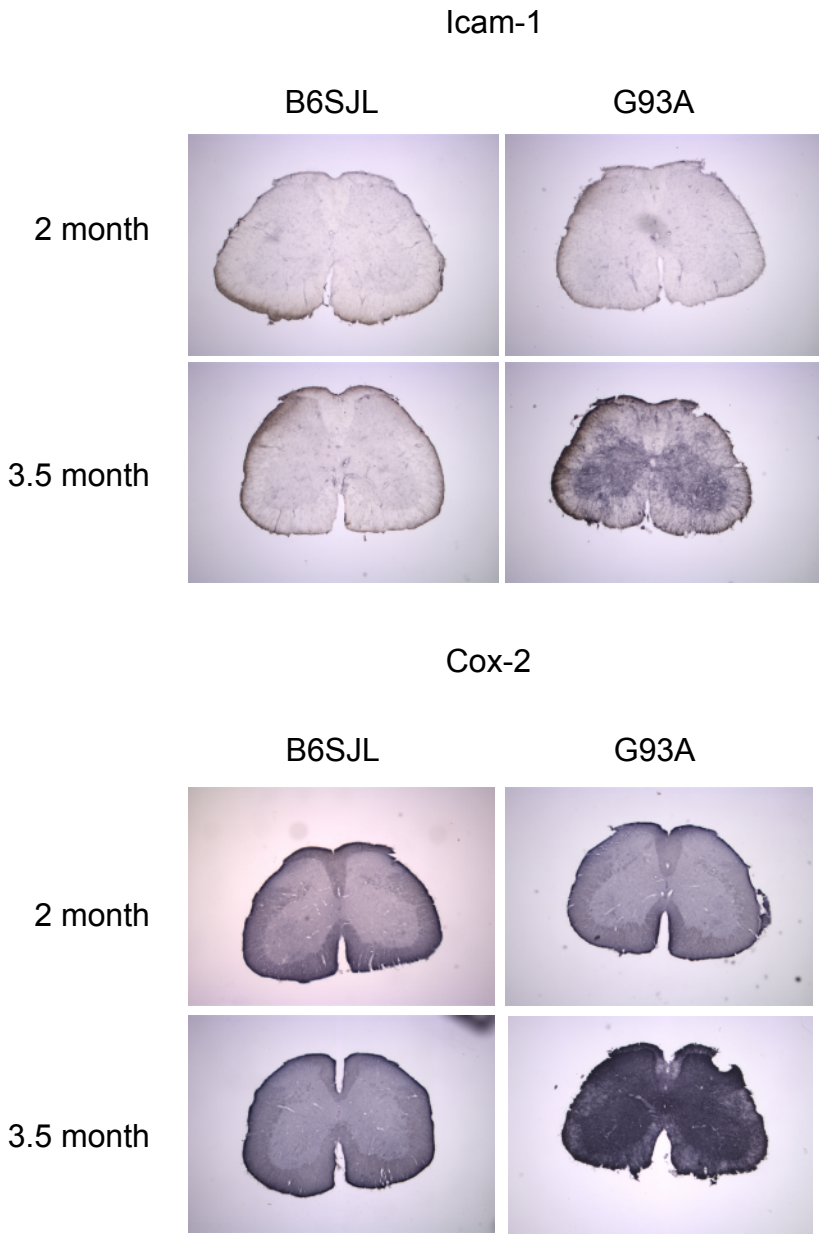

Supplementary Figure 3. Icam-1 and Cox-2 immunostaining in the lumbar spinal cord of SOD1^{G93A} mice at presymptomatic and symptomatic stage.
Representative images of Icam-1 (upper panel) and Cox-2 (lower panel) immunostaining on the lumbar spinal cord sections of SOD1^{G93A} and the age-matched littermate control B6SJL mice at 2 and 3.5 month of age, n = 6 mice per group. The mice were perfused transcardialy with 0.15 M sodium phosphate buffer containing 2 IU/ml heparin and 0.5 % sodium nitrite followed by perfusion with ice cold 4% paraformaldehyde in buffer at pH 7.4. The 30 μm lumbar spinal cord (L2–L4) sections were treated using free-floating method for detecting Icam-1 (1:5,000 dilution, Abd Serotec, Raleigh, NC) and Cox-2 (1:1,000, Cayman Chemical, Ann Arbor, MI). Detection of positively stained tissue was accomplished using the Elite avidin-biotin and 3, 3-diaminobenzidine (Vector Labs) method, as described by the manufacturer.

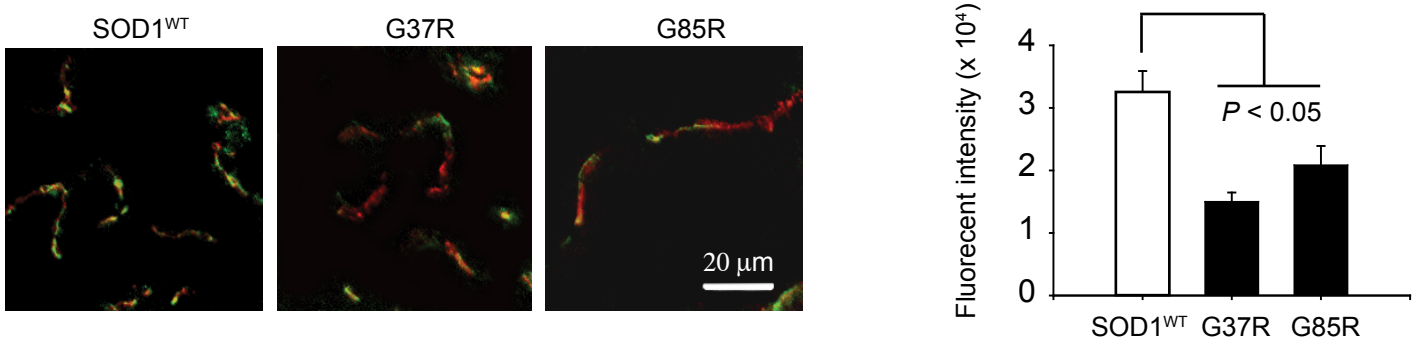

Supplementary Figure 4. ZO-1 and CD31 double immunostaining in the lumbar spinal cord of SOD1^{G37R} and SOD1^{G85R} mice presymptomatically.
ZO-1 (green) and CD31 (endothelial marker, red) double immunostaining in 3.5 months old SOD1^{G37R} mouse and 6.5 months old SOD1^{G85R} transgenic mouse. Merged (yellow) indicates endothelial-associated ZO-1 expression. Findings are representative of 3–5 mice per group. Graph shows relative intensity of the merged (yellow) signal. Means ± s.e.m., n = 3–5 mice per group.

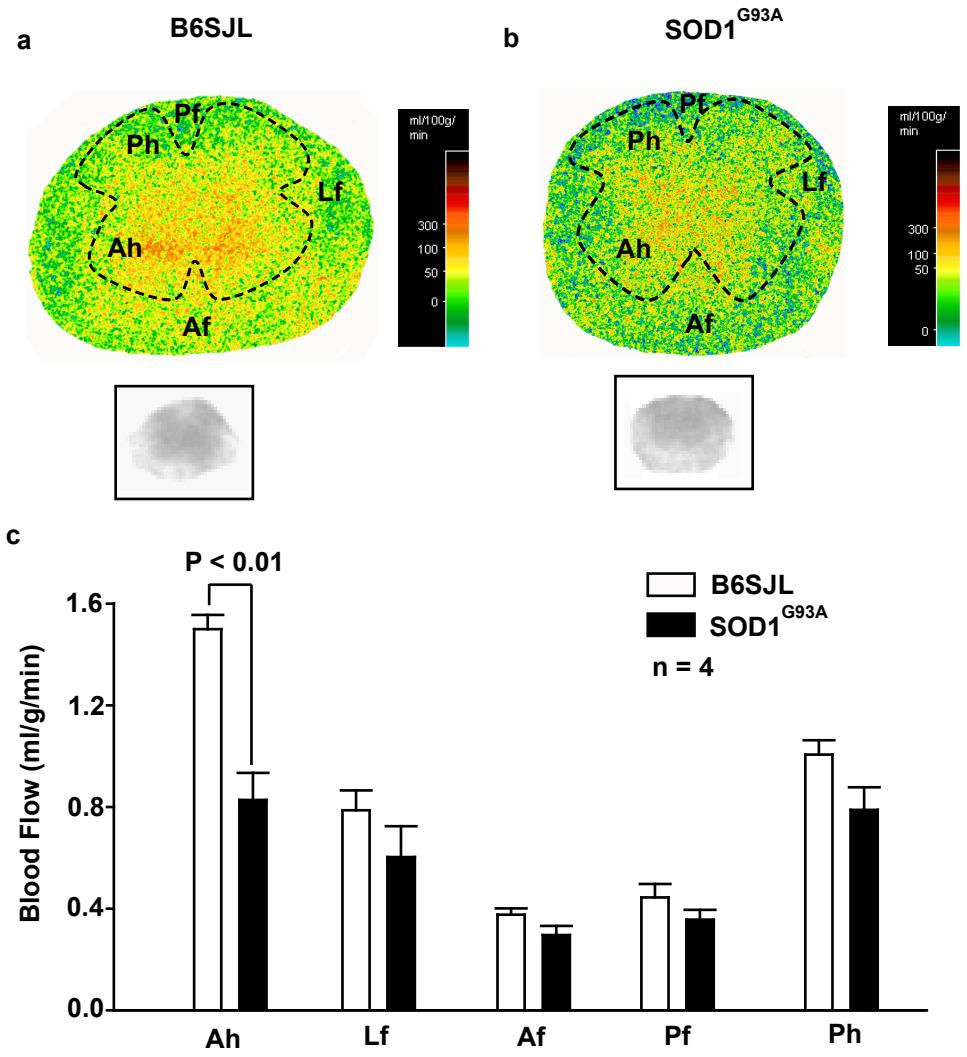

Supplementary Figure 5. Regional blood flow autoradiograms in the lumbar spinal cord of SOD1^{G93A} mice presymptomatically.

Representative autoradiograms of the spinal cord lumbar region (L2) demonstrating blood flow in B6SJL (littermate controls) (a) and SOD1^{G93A} mutant mice (b). (c) Regional blood flow in anterior horn (Ah), lateral funiculus (Lf), anterior funiculus (Af), posterior funiculus (Pf) and posterior horn (Ph) was determined using intraperitoneal ^{14}C-IAP injection and final arterial heart blood sampling, as described[18]. Briefly, we anesthetized mice with 2-3% isoflurane in oxygen (30%) and nitrous oxide (70%) and injected with ^{14}C-IAP (15 µCi, Amersham). Precisely 30 sec after ^{14}C-IAP injection mice were decapitated and quickly immersed in liquid nitrogen until frozen. Blood from the left ventricle of the heart was carefully removed in the cold room (0 ^{o}C) and placed in pre-weighed tubes. Blood samples were decolorized with hydrogen peroxide to reduce quenching, and analyzed for ^{14}C-IAP counts (Tri-carb 2100 liquid Scintillation Counter, PerkinElmer) after dissolving the samples with 0.5 ml tissue solubilizer (PerkinElmer) overnight and adding 5 ml scintillation fluid (Ultima Gold, PerkinElmer). The frozen lumbar region of the spinal cord was carefully removed in the cold room and cryosectioned at 20 µm, mounted on slides, dried on a hot plate at 50ºC for 10 min and exposed to Hyperfilm-βmax autoradiographic film (Amersham) along with ^{14}C standards. After 6 weeks exposure, the film was developed and the resulting images were analyzed on an MCID image analyzer (Imaging research) to determine levels of ^{14}C-IAP in different spinal cord regions by quantitative autoradiography. The local blood flow was calculated with the MCID program. Values are mean ± S.E.M.; n = 4.

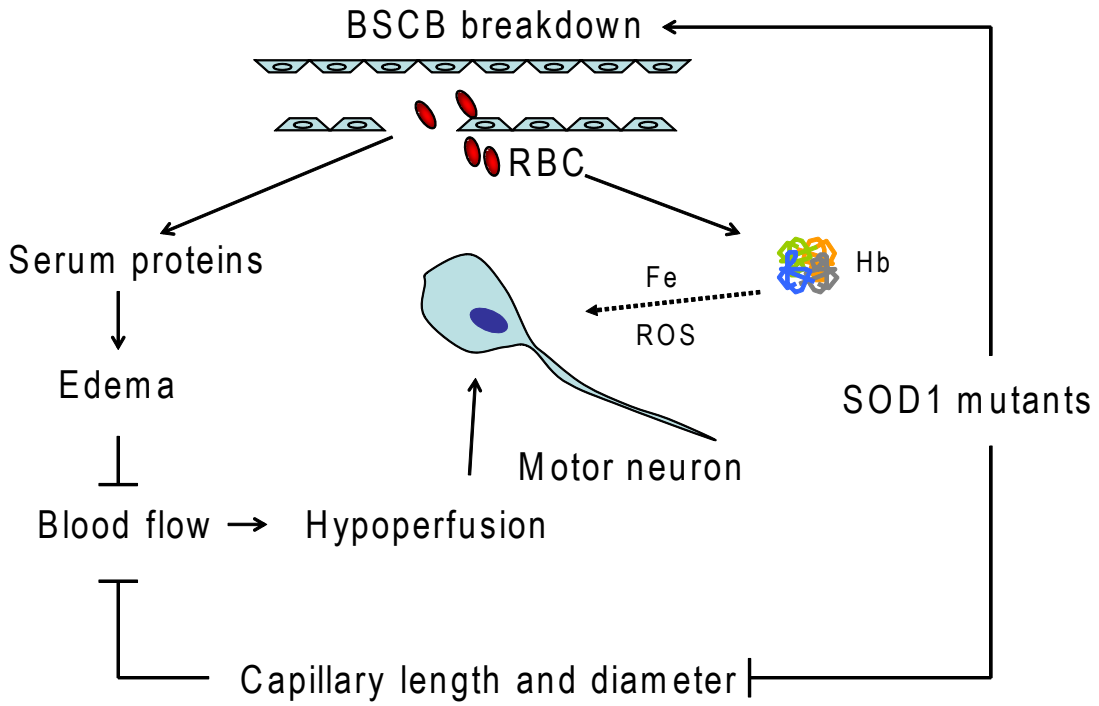

Supplementary Figure 6. Schematic diagram illustrating how direct endothelial toxicity from different SOD1 mutants may result in an early BSCB breakdown and reduction in microcirculation that contributes to motor neuron degeneration.

The BSCB breakdown leads to focal microhemorrhages with leakage of serum proteins and extravasation of red blood cells (RBC). RBC release hemoglobin (Hb) into the spinal cord tissue. Hb is a source of neurotoxic products including free iron (Fe) which catalyzes the formation of toxic reactive oxygen species (ROS) mediating direct neuronal injury. The BSCB disruption and reductions in microcirculation also create a chronic hypoperfusion state aggravating the neuronal injury.

Methods (Supplemental information)

Animals.

Transgenic human SOD1-expressing mice, $SOD1^{WT}$ mice (age of 4 and 7 month)[16], mutant $SOD1^{G37R}$ (age of 3.5 and 5.5 month) and $SOD1^{G85R}$ (age of 6.5 and 11 month)[6] on C57BL6 genetic background were developed in D. W. Cleveland laboratory. Mutant $SOD1^{G93A}$ mice (age of 2 and 3.5 month)[7] F1 hemizygotes on C57BL6 and SJL (B6SJL) background[7] and littermate controls were from the Jackson Laboratory. We also studied wild type littermate control mice. All procedures with SOD1 mutants and wild type mice were according to the NIH guidelines and approved by the University of Rochester Committee on Animal Resources.

Histology and Immunohistochemistry.

For serum protein leakage analysis, Prussian blue staining, MCP-1 immunostaining, ZO-1 immunostaining and total capillary length, mice were anesthetized intrapertioneally with ketamine (100 mg/kg) and xylazine (10 mg/kg) and perfused transcardially with heparinized phosphate buffered saline (PBS). Lumbar spinal cords (L2–L5 region) were embedded in OCT medium (Sacura, Torrens, CA) and cut in the coronal plane at 14 μm. For Icam-1 and Cox-2 immunohistochemistry we used a slightly modified procedure, as described below.

Serum protein leakage. L2–L5 lumbar spinal cord sections (prepared as described above) from littermate controls (3.5 and 12 months old), $SOD1^{WT}$ mice (4 and 7 months old), $SOD1^{G93A}$ mice (2 and 3.5 months old), $SOD1^{G37R}$ mice (3.5 and 5.5. months old) and $SOD1^{G85R}$ mice (6.5 and 11 months old) were analyzed for serum protein leakage using anti-serum protein (IgG) antibodies (n = 3–5 mice per group). Sections were fixed in acetone for 5 min, blocked by 5% swine serum for 1 h at room temperature, and incubated with fluorescein-conjugated affinity purified goat anti-mouse IgG (fluorescein-labeled primary antibody; 1:200, Jackson Immuno Research, West Grove, PA) and rat monoclonal anti-mouse CD31 (endothelial marker; 1:100, BD Pharmingen, San Diego, CA) overnight at 4°C. The sections were then washed with PBS and incubated with AlexaFluor 594 donkey anti-rat IgG (secondary antibody to CD31 antibody; 1:200, Molecular Probes, Eugene, OR) for 1 h at room temperature. Images were taken using an Olympus AX70 fluorescent microscope. Twelve nonadjacent sections (> 250 μm apart in the L2-L5 region) were examined in each mouse and the fluorescent intensity of mouse IgG extravascular deposits was analyzed using Image-Pro Plus software (Media Cybernetics, Inc, Silver Spring, MD). Sections of all control and experimental mice were processed in parallel.

Prussian blue staining. We used a standard procedure. Briefly, acetone fixed L2-L5 lumbar sections from littermate controls (3.5 and 12 months old), $SOD1^{WT}$ mice (4 and 7 months old), $SOD1^{G93A}$ mice (2 and 3.5 months old), $SOD1^{G37R}$ mice (3.5 and 5.5. months old) and $SOD1^{G85R}$ mice (6.5 and 11 months old) (n = 3 – 5 mice per group) were incubated in a 5% potassium ferrocyanide and 5% hydrochloric acid solution (1:1

working solution) for 30 min. The sections were then washed and subsequently counterstained with nuclear fast-red. Hemosiderin shows blue, the nuclei show red, whereas the cytoplasm shows pink. Twelve nonadjacent sections (> 250 μm apart in the L2–L5 region) were examined in each mouse and the total number of spots positive for hemosiderin was determined. To access the relative abundance of Prussian blue positive deposits per section, we divided total numbers of Prussian blue positive spots by the number of studied sections.

MCP-1 immunostaining. L2–L5 lumbar spinal cord sections from age-matched littermate controls and $SOD1^{G93A}$ mice at 2 and 3.5 months of age (n = 4 mice per group) were fixed in acetone for 5 min, blocked by 5% swine serum for 1 h at room temperature, and incubated with goat polyclonal anti-mouse MCP-1 (1:100, Santa Cruz Biotechnology) overnight at 4°C. The sections were then washed with PBS and incubated with AlexaFluor 488 anti-goat IgG (1:200, Molecular Probes, Eugene, OR) for 1 h at room temperature. Images were taken using an Olympus AX70 fluorescent microscope. Twelve nonadjacent sections (> 250 μm apart in L2–L5 region) were examined in each mouse. All sections from control and experimental animals were processed in parallel.

ZO-1 immunostaining. L2-L5 lumbar spinal cord sections (prepared as described above) from littermate controls (3.5 and 12 months old), $SOD1^{WT}$ mice (4 and 7 months old), $SOD1^{G37R}$ mice (3.5 months old) and $SOD1^{G85R}$ mice (6.5 months old) were analyzed for ZO-1 staining intensity (n = 3–5 mice per group). Sections were fixed in acetone for 5 min, blocked by 5% swine serum for 1 h at room temperature, incubated with rabbit polyclonal anti-mouse ZO-1 (1:500, Invitrogen, South San Francisco, CA) and rat monoclonal anti-mouse CD31 (1:100, BD Pharmingen, San Diego, CA) antibodies overnight at 4°C. After washing with PBS the sections were incubated with AlexaFluor 488 donkey anti-rabbit IgG (1:200, Molecular Probes, Eugene, OR) and AlexaFluor 594 donkey anti-rat IgG (1:200, Molecular Probes, Eugene, OR) for 1 h at room temperature. Images were taken using an Olympus AX70 fluorescent microscope. Twelve nonadjacent sections (> 250 μm apart in the L2–L5 region) were examined in each mouse. The fluorescent intensity of the ZO-1 signal was analyzed using Image-Pro Plus software (Media Cybernetics, Inc, Silver Spring, MD). Sections of all control and experimental animals were processed in parallel.

Total capillary length. L2–L5 lumbar spinal cord sections (prepared as described above) from littermate controls (3.5 and 12 months old), $SOD1^{WT}$ mice (4 and 7 months old), G93A mice (2 and 3.5 months old), G37R mice (3.5 and 5.5. months old) and G85R mice (6.5 and 11 months old) were analyzed for total capillary length (n = 3–5 mice per group). Sections were fixed in acetone for 5 min, blocked by 5% swine serum for 1 h at room temperature, and incubated with rat monoclonal anti-mouse CD31 (1:100, BD Pharmingen, San Diego, CA) overnight at 4°C. Sections were then washed with PBS and incubated with AlexaFluor 594 donkey anti-rat IgG (1:200, Molecular Probes, Eugene, OR) for 1 h at room temperature. Images were taken using an Olympus AX70 fluorescent microscope. Twelve nonadjacent sections (> 250 μm apart in the L2–L5 region) were examined in each mouse. The total length of CD31-positive blood vessels in the anterior horn was determined using Image-Pro Plus software (Media Cybernetics, Inc, Silver

Spring, MD). Total capillary length was expressed as the total length in mm of CD31-positive vessels per unit area in mm^2. Sections from control and experimental animals were processed in parallel.

Icam-1 and Cox-2 immunochemistry. $SOD1^{G93A}$ mice (age of 2 and 3.5 month) and age-matched littermate controls (n = 6 mice per group) were anesthetized as described above. Animals were perfused transcardially with 0.15 M sodium phosphate buffer containing 2 IU/ml heparin and 0.5 % sodium nitrite followed by perfusion with ice cold 4% paraformaldehyde in buffer at pH 7.4. The lumbar region of the spinal cord was removed and postfixed for 24 h. Tissue was equilibrated overnight in 0.15 M phosphate buffer containing 30% sucrose, quick frozen in isopentane, and stored at –80 °C. 30 μm sections were cut on a sliding knife microtome using a –25 °C freezing stage. The free floating sections were stored in cryoprotective solution at –20 °C until further processing.

Sections were treated using free-floating method for detecting Icam-1 (1:5000 dilution, Serotec) and Cox-2 (1:1000 dilution, Cayman) protein. Detection of positively stained tissue was accomplished using the Elite avidin-biotin and 3,3-diaminobenzidine (Vector Labs) method. After extensive rinsing of the sections and blocking of the endogenous peroxidase by incubation for 20 min in 3% hydrogen peroxide, the sections were placed in 10% normal goat serum in PBS for 1 h. After this step, we incubated the sections with the primary antibody in 0.15 M phosphate buffer containing 1% normal serum and 0.4% triton X-100 for 24–48 h at 4°C. After extensive rinsing, the tissue was incubated with biotinylated secondary antibody for 2–3 h. The staining was concluded by the peroxidase reaction in a solution containing 0.05% 3,3-diaminobenzidine, 0.125 M sodium acetate, 10 mM imidazole, 0.1 M nickel sulfate, and 0.03% hydrogen peroxide. The development was observed visually and terminated with rinses in water. To limit variability between separate staining procedures, sections of all experimental and control groups were processed in parallel.

Real-time quantitative RT-PCR.

$SOD1^{G93A}$ mice (age of 2 and 3.5 month) and age-matched littermate controls (n = 6 mice per group) were anesthetized as described above. Upon cessation of any reaction to nociceptive stimuli, the animals were decapitated and the spinal cord was removed by flushing the tissue from the spinal canal. The lumbar region was dissected out of the spinal cord and immediately quick-frozen by placing it into a solution of isopentane on dry ice. The tissue was stored at –80 °C until ready for RNA extraction. Subsequently, RNA was isolated using TRIzol reagent (Invitrogen Life Technologies), precipitated, treated with DNase I, and quantified using a spectrophotometer. Following quantification of the RNA, 1 μg of the final product underwent reverse transcription utilizing Superscript III reverse transcriptase (Invitrogen Life Technologies) and random hexamer primers. The cDNA product of the RT reaction was stored at –20 °C or used immediately for the Q-PCR.

For quantification of *MCP-1*, *Cox-2* and *Icam*-1 mRNA levels, we used primers and FAM 490 probes (Biosearch Technologies) custom designed using the Oligo 6.0 software program (Molecular Biology Insights, Inc.) for implementation in the iCycler iQ™ Real Time PCR Detection System by Bio-Rad. Prior to amplification of the cDNA

samples, reaction conditions were empirically optimized for each experimental gene. Melt curve analysis for each PCR amplification cycle was also conducted in order to confirm synthesis of a single product with the expected melting temperature. The standard curves were generated by using a serial dilution over 5 orders of magnitude of either one of the samples or cDNA of a spleen from a lipopolysaccharide-treated mouse, which demonstrates a robust level of expression of pro-inflammatory markers. We used the iCycler IQ software, version 3.0a, to analyze the efficiency of reactions.

PCR reactions were carried out in a final volume of 25 μl containing iQ Supermix® (Bio-Rad), 5 nM FITC dye, and 1 μl of the cDNA sample. We employed these reaction conditions: denaturation at 95°C for 3 min, followed by 50 cycles of amplification that include denaturing at 95°C for 30 sec, annealing for 30 sec, and extension at 72°C for 1 min. Annealing temperatures were specific for each gene product and were established by prior optimization procedures described above. PCR products were monitored using FAM 490 fluorescence during the last 10 sec of each extension step. Results were expressed as the number of cycles required to reach threshold (the start of the exponential phase of amplification). Threshold cycle (Tc) values were transformed using the function Expression = $(1+E)^{Tc}$ in order to determine relative differences in mRNA expression. Glyceraldehyde-3-phosphate dehydrogenase (GAPDH), a housekeeping gene, was used as an internal control to normalize the amount of cDNA for each experimental sample.

Immunoblotting of spinal cord microvessels.

We isolated spinal cord microvessels from $SOD1^{G93A}$, $SOD1^{G37R}$ and $SOD1^{G85R}$ mice at 2, 3.5 and 6.5 months of age, respectively, $SOD1^{WT}$ mice at 7 months of age, B6SJL and C57BL/6 control mice at 2 and 7 months of age, respectively, as described[17]. Spinal cords from three to five mice (n = 3–5 mice per group) were pooled. We conducted three independent experiments. Microvessels were lysed in the Cell Lysis Buffer (Cell Signaling Technology, Danvers, MA). Twenty μg of proteins were used for analysis by 10% SDS/PAGE, and subsequently transferred to nitrocellulose membrane. This membrane was then blocked for 1 h with 5% non-fat milk in tris-buffered saline. Then the membrane was washed and incubated with a horseradish peroxidase-conjugated secondary antibody for 1 h. Reactivity was detected by using an enhanced chemiluminecence detection system (Amersham, Piscatawaym, NJ). We used the following primary antibodies: goat polyclonal anti-human beta-actin which cross reacts with mouse actin (1:1,000, Santa Cruz Biotechnology, Santa Cruz, CA), goat polyclonal anti-human ZO-1 which cross-reacts with mouse ZO-1 (1:250, Santa Cruz Biotechnology, Santa Cruz, CA), mouse monoclonal anti-mouse occludin (1:50, BD Biosciences, San Jose, CA), rabbit polyclonal anti-claudin-5 (1:50, Novus, Littleton, CO), goat polyclonal anti mouse Glut-1 antibody (1:200, Santa Cruz Biotechnology, Santa Cruz, CA), goat polyclonal anti-human SOD1 (1:100, Santa Cruz Biotechnology, Santa Cruz, CA), rabbit polyclonal anti-mouse SOD1 (1:200, Chemicon, Temecular, CA). Mouse SOD1 was blotted on the same blot as the human SOD1 after human SOD1 was partially stripped off. The density of bands for ZO-1, hSOD1, mSOD1 and Glut-1 was quantified by using scanning densitometry relative to β-actin signal (Alpha Imager,

Alpha Inotech, San Leandro, CA). For each studied protein signal was within the linear range.

Electron Microscopy.

$SOD1^{G93A}$, $SOD1^{G37R}$ and $SOD1^{G85R}$ mice at 2, 3.5 and 6.5 months of age, respectively, and age-matched littermate controls (n = 3–4 mice per group) were anesthetized intrapertioneally with ketamine (100 mg/kg) and xylazine (10 mg/kg) and perfused transcardially with (30 mL) heparinized 0.9% saline, followed by (50 mL) 4.0% paraformaldehyde (PFA) and 1.0% glutaraldehyde. The cervical and lumbar spinal cords were carefully dissected and post-fixed in 4.0% PFA and 1.0% glutaraldehyde overnight, then sectioned at 75 μm on a Vibratome. The sections were rinsed in tris (hydroxymethyl) aminomethane (Tris) buffer (pH = 7.4), post-fixed in 1.0% osmium tetroxide, and infiltrated in Spurr epoxy resin and embedded. The resin embedded tissue was polymerized at 70 ^{0}C overnight. Semi-thin (1.0 μm) spinal cord sections were cut with a glass knife to select the anterior horn area for ultra-thin sectioning with a diamond knife. Sections were placed on grids, stained with uranyl acetate and lead citrate, and examined by a Hitachi (Tokyo) 7100 electron microscope. Neuronal and microvasculature morphology was characterized utilizing standard ultrastructural criteria and images were captured using a Megaview III digital camera (Soft Imaging System, Lakewood, CO).

Measurements of blood flow in brain and spinal cord.

Blood flow to the brain (cortex) and spinal cord lumbar and cervical regions of the spinal cord was determined using ^{14}C-iodoantipyrine (IAP) in 2 months old $SOD1^{G93A}$ mice and age-matched littermate controls (n = 4 mice per group) by combining intraperitoneal (i.p.) tracer application with a single blood sampling from the heart at the end of experiment, as described[18]. The i.p. method for cerebral blood flow measurements is much simpler than the intravenous (i.v.) ^{14}C-IAP infusion method, and has been validated in our laboratory (Maness LM, Maurer CR, LaRue BA, Welch DM, Zlokovic BV (2001) Simultaneous measurement of cerebral blood flow and blood-brain barrier permeability in the anesthetized mouse Soc Neurosci Abstracts 27, 1391). The i.p. method offers several advantages compared to the i.v. ^{14}C-IAP infusion method which is complicated in mice, especially in transgenic models, because (i) it requires the cannulation of several blood vessels (i.e., arterial lines for blood sampling and blood pressure monitoring and a venous line for tracer infusion) which demands precise and long-lasting microsurgery under general anesthesia; and (ii) there is a loss of blood during repeated arterial sampling which may lead to hemorrhagic hypotension and compromise the physiological status of the animal.

We confirmed there was no a significant difference in blood flow measurements conducted in mice using either the i.p. or the i.v. method, as previously reported[18]. The differences in blood flow values through the cortex, cervical and lumbar cord of C57BL6 mice calculated by the two methods differed between 6 and 9%, which was not significant, as reported[18].

SOD1^{G93A} mutant mice and age-matched littermate control mice were anesthetized by 2–3% isoflurane in 30% oxygen and 70% nitrous oxide. ^{14}C-IAP (Amersham;15 μCi in 100 μl saline) was administered i.p. After 30 s anesthetized mice were decapitated and the head and rest of the body were rapidly frozen in liquid nitrogen. There was a 3 s delay of ^{14}C-IAP entry into the blood after the i.p. injection (lag time), as reported[27]. We also confirmed in a separate group of mice (n = 3), that the appearance of ^{14}C-IAP in the blood after the i.p. administration remains linear within 60 s, as reported[18]. Frozen brain (frontal cortex) and spinal cord (cervical and lumbar) regions were carefully dissected in the cold room (0 °C), placed into pre-weighed vials and prepared for radioactivity analysis. Frozen blood from the left ventricle of the heart was also removed in the cold room (0 °C) and prepared for counting. Blood samples were decolorized with hydrogen peroxide to reduce quenching. Blood, spinal cord and cortical tissue samples were dissolved in 0.5 ml tissue solubilizer (PerkinElmer) overnight, and analyzed for ^{14}C-IAP radioactivity (Tri-carb 2100 liquid Scintillation Counter, PerkinElmer) after adding 5 ml scintillation fluid (Ultima Gold, PerkinElmer).

Calculation. Blood flow, F (ml/g/min) through the spinal cord lumbar and cervical spinal cord regions and cortex was determined by using the equation, as described[18].

$F = \lambda/T \ln (1- C_I(T)/\lambda \ {}_0\int^T C_A(T)$, where $C_I(T)$ is ^{14}C-IAP radioactivity (d.p.m.)/gram of spinal cord or brain tissue; T is the experimental time in seconds; $C_A(T)$ is ^{14}C-IAP radioactivity (d.p.m.)/gram plasma determined as ^{14}C-IAP integrated plasma concentration (${}_0\int^T$) from ^{14}C-tracer lag time after ^{14}C-IAP i.p. injection (zero time) to the value measured in the blood sample from the frozen heart at the end of the experiment (at time T), by assuming a linear rise or ramp function over T; λ is ^{14}C-IAP central nervous system tissue to blood partition coefficient, 0.8 ml/g.

Autoradiography. Prior to preparing lumbar regions for tissue radioactivity counting, the frozen cord was cryosectioned at the L2 level at 20 μm, mounted on slides, dried on a hot plate at 50 °C for 10 min and exposed to Hyperfilm-βmax autoradiographic film (Amersham) along with ^{14}C standards. Blood flow through the anterior horn and other regions of the gray and white matter (n = 4 mice per group) was calculated as described[18]. For details see Supplementary Fig. 5.

Statistical analysis.

Data from different samples were analyzed using methods of distribution statistics (standard descriptive analysis), by analysis of the means (Student *t*-test) and by an analysis of variance (ANOVA). A probability of $P < 0.05$ was considered significant. All values were mean ± s.e.m.

16. Wong, P.C. *et al.* An adverse property of a familial ALS-linked SOD1 mutation causes motor neuron disease characterized by vacuolar degeneration of mitochondria. *Neuron* 14, 1105–1116 (1995).

17. Wu, Z., Hofman, F. & Zlokovic, B.V. A simple method for isolation and

characterization of mouse brain microvascular endothelial cells. *J. Neurosci. Meth.* **130**, 53–63 (2003).

18. Maeda, K., Mies, G., Oláh, L. & Hossmann, K.-A. Quantitative measurement of local cerebral blood flow in the anesthetized mouse using intraperitoneal [14C]iodoantipyrine injection and final arterial heart blood sampling. *J. Cereb. Blood Flow & Metab.* **20**, 10–14 (2000).